Future Cities and Environment
ISSN 2363-9075 Volume 12 (2026)

https://doi.org/10.70917/fce-2026-004
Article

Single-Family Wooden House That Chases the Sun and Saved Energy

Gianfranco Castrovinci [1,*] and Mercedes Galiana [2]

[1] Tecnologías de la Computación e Ingeniería Ambiental, UCAM Universidad Católica de Murcia, 30107 Murcia, Spain
[2] Department of Architectural Constructions, Universitat Politècnica de València, 46022 Valencia, Spain
* Correspondence author: gcastrovinci@alu.ucam.edu

Abstract: For several decades now, the energy problem has been a matter of vital importance, both for the very existence of human beings and for that of our planet. Real solutions are based on energy savings and energy production through renewable energy sources (RES). The building industry, with consumption corresponding to about 40% of global energy needs, is a sector of great interest for which to develop such solutions. This article aims to present a study relating to the actual energy gains that can be obtained from the construction of solar-tracking buildings. The study was conducted by taking into consideration a standard single-family timber building, with a rectangular geometry and a flat roof, and making calculations in correspondence for 21 Italian locations. This article presents the results of the 11 sites that best represent the different climatic conditions present in Italy. Starting from astrophysics and heat transfer studies, it has been demonstrated that the rotation of a building with a speed equal to the apparent speed of the Sun, characterized by appropriate angles of incidence of the rays depending on the different climatic conditions encountered during the year, makes it possible to obtain energy gains of great interest, both in the autumn-winter heating phase and in the spring-summer cooling phase, without compromising the conventional techniques used in the energy-saving sector. In addition, further energy increases are obtained by photovoltaic and solar-thermal systems, located on the roof of the structure.

Keywords: energy saving; energy efficiency; solar tracking buildings; wooden house; building orientation

1. Introduction

The availability of energy is one of the main conditions for the development of a society.

Unfortunately, most of global production worldwide originates from fossil fuels which, therefore, are consumed millions of times faster than the rate at which they formed, by virtue of very slow natural processes, and therefore are destined to be progressively depleted. In particular, oil reserves amount to about 237 · 109 t (Our World in Data, 2020), those of gas to about 188 · 1012 m^3 (Our World in Data, 2020) and those of coal to about 1,074 · 109 t. Corresponding to these reserves there are the following annual consumption levels: 55,292.08 TWh for oil (Our World in Data, 2020), 41,278 TWh for gas (Our World in Data, 2020) and 45,850 TWh for coal (Our World in Data, 2020). At present, oil is expected to run out in about 56 years, gas in about 49 years, and coal in about 139 years (Our World in Data, 2020).

Another problem arises from the fact that the most important deposits are in specific geographical areas, not all of which are geopolitically stable, therefore it can be deduced that the tensions and conflicts connected with energy sources may become increasingly acute. In addition, there is the possibility of using the availability of raw materials as a source of blackmail in the management of politico-military disputes (DIIS, 2024).

To aggravate these conditions, there is the fact that the same fuels have been shown to be the primary cause for the environmental degradation, with serious consequences on human health, fauna, flora and artistic heritage: the intensification of extreme meteorological phenomena and the damage they produce is widely observed. There are countless studies that have addressed the problem, particularly in highly

developed countries, analysing the current state and policies to improve present and future conditions (Zhu, 2025).

The latest IPCC report (IPCC, 2023) underscored the need for action by all nations to reduce their emissions. This requires investments in renewable energy sources (RES), in technologies and techniques that reduce greenhouse-gas emissions as much as possible.

Over time, in addition to improving technologies within renewable energy sources (RES), more and more original interventions have been identified such as, for example, solar dynamic-control devices (Carbonari, 2025) and passive strategies (Suman, 2025). Other studies have addressed broader aspects that include areas related to various needs, such as, for example, energy saving and people's well-being (Zhang, 2025). In the construction sector, with varying fortunes, we have gone from overly restrictive measures, particularly during the oil crises of the 70s (1970s), to a more balanced search for solutions linked to a different vision of design, increasingly projected towards energy saving considered not only in its specificity, but also in all aspects of life to which it is closely linked.

Abandoning attitudes that, for a long time, have been more a matter of fashion, disguised as ethical issues, than a concrete ability and will to address, over time we have arrived at solutions that, in many cases, even if they appear as a distortion of common design, have actually represented insights and improvements of visions that have evolved over the years.

Far from seeking a description of the evolution in design of the last hundred years, it is appropriate to point out the key points of this evolution.

The main actors of the Modern Movement, such as Mies Van der Rohe, Le Corbusier, Gropius, although in the diversity of the various components which, however, interacted by influencing each other, freed themselves from anachronistic formal constraints, turning their attention to the real needs of the historical moment in which they lived, such as social, functional and practical needs, with design directed toward addressing them. The elements of convergence between the various components had been well codified by Bruno Taut in "Modern Architecture" (Taut, 1929).

The next phase, post-war, represented a reversal of the revolutionary vision of the previous phase, moving design away from genuine human needs (Arieti, 2021). This trend has become more acute over the years to the point that it became a matter reserved for an elite, increasingly devaluing the architecture itself and abandoning the search for solutions to the need for building functionality (Arieti, 2021).

Over the years, the environmental emergency has increased, to the point of becoming an absolute priority today. While not renouncing aesthetic requirements, the need to link the latter to the concept of functionality that a building must have, with technical choices that go in this direction, has become essential. In the face of the tendency in some contexts to solve energy problems by limiting themselves to the use of renewable energy sources (RES) alone, the evolution of choices has been correctly oriented towards the study of the building envelope. Technologies that rely on the production of energy from renewable sources have been relegated to guaranteeing the energy needs of a building, once losses have been limited as much as possible (Arieti, 2021; E.U., 2021). The design, in addition to the usual architectural needs, was aimed at solving specific problems related to energy efficiency, such as the elimination of thermal bridges, thermal insulation, airtightness, integrated design processes. In addition to all this, particular attention was added, in the construction phase, to the installation of specific components, in order to prevent imperfect construction from leading to losses not anticipated during the design phase.

Together with the aforementioned experiences, concerning both the architectural-functional aspects and those relating to energy efficiency, particular experiments have been carried out over the years such as the construction of rotating buildings.

The first concrete case was realised in Italy between 1929 and 1935. This is Villa Girasole (Figure 1), located in Mezzavilla di Marcellise (VR), built in the Art Deco style. It was designed by the engineer Angelo Invernizzi, assisted, in some respects, by the architect Ettore Fagiuoli, as a holiday home (Galfetti, 2014).

It was not particularly successful because the idea behind its construction clashed with a more classical vision of architecture, as it privileged the dominance of technology and amplifying the contrast between old and new principles that characterized the idea of a building, in particular between stillness and movement.

The idea of its creator was to free himself from the weight of the old structures to pursue a new relationship with the environment, space, and time.

In addition, the innovative "V" (Figure 2) shape allowed outside observers a perception of concavity or convexity depending on their position and the moment at which they looked at the building and, at the same time, the building’s occupants inside Villa Girasole, to experience two diametrically opposed sensations provided by the particular landscape of Marcellise: a wide valley on one side and a hilly environment, enclosed and intimate, on the other.

Figure 1. Villa Girasole – 1935 c., Source: (Galfetti, 2014).

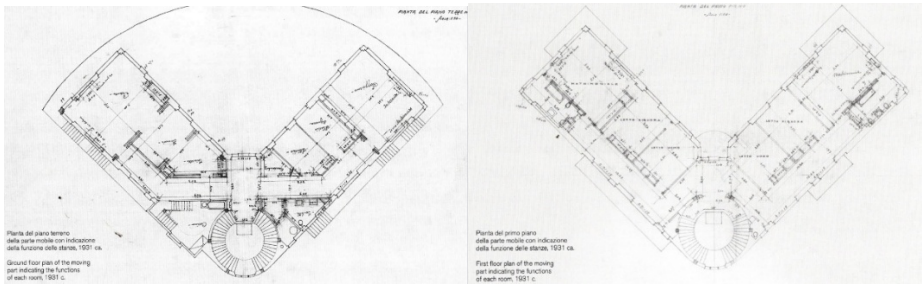

Figure 2. Ground and first plan – 1931 c. Source: (Galfetti, 2014).

It should also be noted that, although not directly addressed at that time, the project of the engineer Invernizzi anticipated, at least at the level of idea, the environmental needs, today increasingly impossible to defer, presented previously.

Over time, other experiences of this type have been carried out. Just to name a few: the "D'Angelo House", built in 1963 in the Snow Creek area near Palm Springs, California (USA); "The Round House", built in 1968 near Wilton, Connecticut (USA); the "Rotating Girasole Home", completed in 2013 in the suburbs of Canberra (Australia); the "Quadrant House", in the suburbs of Warsaw (Poland); the "Heliotrope", in Freiburg (Germany); the "Sharifi-ha House", in Tehran (Iran); the "Kiefer Technic Showroom", Bad Gleichenberg (Austria); the "Kuggen" in Göteborg (Sweden); the "Suite Vollard", Curitiba (Brazil); the "Rotating House" in San Diego, California (USA).

In particular, the D'Angelo House, the Round House, the Rotating Girasole Home, the Heliotrope, Vollard Suite and the Rotating House are real rotating buildings or apartments, the rest are not rotating houses but architectures whose mobile skin responds to the Sun; the others are not rotating buildings but architectural designs whose movable skin responds to the sun.

Figure 3 presents the previous buildings in a collage, in the order just indicated.

Figure 3. Various examples of rotating buildings, Sources: (a) (Ward, 2012), (b) (Bahan, 2016), (c) (Eve, 2014), (d) (Ottolenghi, 2025), (e)–(i) (Cerizzi, 2024), (l) (McLaughlin, 2023), Edited by: Researches.

Another aspect addressed in relation to the building envelope was that connected to the so-called Adaptive Dynamic Building Envelopes (ADBEs), capable of integrating different technologies and components in order to improve the performance of a building (Nagy, 2022).

Starting from these experiences, particularly those involving rotating buildings, the study of the present project has turned its attention not to merely panoramic issues but to the real possibility of contributing to building energy savings.

Therefore, studies carried out over the years by researchers, such as Liu-Jordan, Page, Klein, Iqbal, and Lazzarin, just to name a few, based on the calculation of the energy due to solar energy incident on a surface, have been taken into consideration. The purpose of these studies is driven by various factors, minimizing energy demand for space heating and cooling, and maximizing the energy that can be produced by photovoltaic and solar thermal panels.

For this purpose, starting from studies based on spherical geometry, we arrived at the determination of an angle θ, called the angle of incidence, defined as the angle between the solar rays and the perpendicular to a given surface (Iqbal, 1983).

By correlating the solar constant I_{CS} (1.367 W m^{-2}) with this angle, it is possible to determine the value of the intensity of solar radiation I_0 incident on any fixed surface, located outside the Earth's atmosphere, whatever its position and its orientation (Lazzarin, 1981; Duffie, 2013):

$$I_0 = r \cdot I_{CS} \cdot \cos(\theta) \text{ [W m}^{-2}\text{]} \quad (1)$$

where r is the Sun-Earth distance (Lazzarin, 1981).

The optimal inclination of a fixed system depends on the specific needs for which the system itself was designed. The conditions change depending on its function. For example, the need to heat a room will be limited to the winter period whereas electricity or thermal energy production typically extends throughout the year.

The angle of incidence makes it possible to carry out evaluations of this type in relation to the direct component of the solar rays.

Many studies have led to results that take into account the passage of solar rays within the Earth's atmosphere, allowing the determination of not only the direct component but also the diffuse and reflected components (Goswami, 2015).

In particular, Hottel's model (Hottel, 1976) allowed the determination of the direct radiation τ_b on clear or cloudy days for four types of climates (Cucumo, 1994; Grassi, 2015).

For diffuse radiation at ground level on a horizontal plane, Liu and Jordan developed an empirical relation that allows the diffuse transmission coefficient τ_d to be calculated once the direct transmission coefficient τ_b is known (Liu, 1960).

As an alternative to these models, when experimental data are available on the monthly mean values of the daily radiation incident on the horizontal surface, $\overline{H}$, it is possible to proceed using the model proposed by Liu-Jordan (Liu and Jordan, 1961) or that of Page (Page, 1961).

By determining specific factors, such as R_b, for the conversion from horizontal surface to inclined surface, and the cloudiness index $\overline{K}_h$, it is possible to calculate the value of the components of the radiation incident on a surface regardless of its orientation within the Earth's atmosphere: the direct ($H_{b\beta}$), the diffuse coming from the celestial sphere ($H_{d\beta}$), and the diffuse coming from the ground reflection ($H_{r\beta}$) (Lazzarin, 1980).

The sum of these three components will give the total value of the radiation incident on the inclined surface.

These evaluations can be performed both for specific days of the year, and with reference to average values of a month (Iqbal, 1983).

Things become enormously complicated in the case of a surface azimuth angle different from zero (walls not facing the equator), both for the determination of the sunrise and sunset angles and for the calculation of R_b.

For the general case, Klein extended Liu and Jordan's method to calculate R_b. (Klein, 1977).

These relations allow this physical quantity to be calculated under certain conditions (it is not possible to determine its values in particular cases such as, for example, for vertical walls, or walls oriented to the east or west).

The general scientific objective of the research project is to identify the conditions and physical-technical parameters of solar gains on the facades of a wooden house with dynamic solar tracking, in order to minimise energy consumption. Therefore, the project aims to develop a method to determine the energy gains achievable through rotating buildings that follow the Sun's apparent motion.

2. Methodology

Starting from the previous premises, within the study initially presented, a method was developed for the determination of the energy gains that can be obtained through the construction of appropriate rotating buildings with reference to the apparent motion of the Sun. In particular, a house made of wood (150 m^2, 450 m^3) with a rectangular base and a flat roof was considered. Wood was chosen for a number of reasons, in particular for its sustainability (its use in construction is less energy-intensive than many other materials, waste can be used for other products or to produce energy, just as it is possible to reuse the material at the end of the structure's life cycle), for its reduced weight given its load-bearing capacity (the strength-to-weight ratio of structural wood is about 20% higher than that of structural steel and more than four times that of unreinforced concrete) (Mazzucchelli, 2016), for its strength and flexibility, for its insulation characteristics (thermal conductivity λ between 0.13 and 0.18 W/m°K) (Thomas Schrentewein, 2008).

As regards sustainability, a parameter of particular importance is that associated with CO_2e emissions. It should be noted that 1 m^3 of wood stores approximately 250 kg of carbon, which corresponds to about 1 t of CO_2. In light of this, and considering the key role of trees (and therefore wood) in carbon regulation, it is worth noting that producing 1 t of cement releases approximately 1 t of CO_2 into the atmosphere; producing 1 t of concrete releases about 0.8 t of CO_2 (without considering the additional issue of water consumption). For 1 t of steel, approximately 1.8 t of CO_2 are generated; for copper, emissions amount to about 3.3 t CO_2e per tonne of product; and for glass, about 0.57 t CO_2e per tonne of glass.

It is therefore evident that construction using solid wood panels offers opportunities for carbon engineering, for example by transforming buildings, and even entire districts, into "carbon sinks".

Finally, the strong suitability of this material for prefabrication offers significant advantages in construction-site organization, reducing on-site work and enabling a substantial reduction in execution times. For these reasons, it is clear why wood has been used as a construction material for thousands of years.

Figure 4 shows the plan and the corresponding elevation of the model considered in this study.

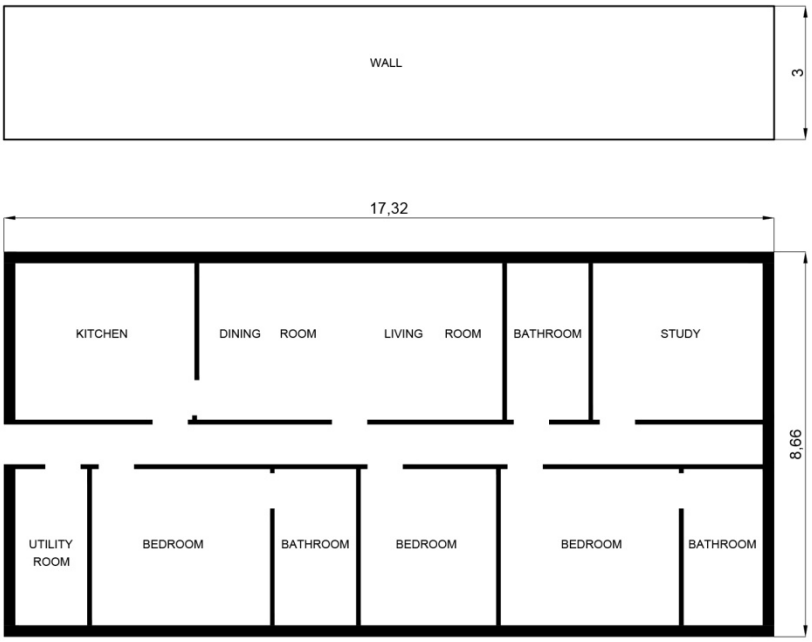

Figure 4. Plan and elevation of the house model considered.

This first assessment would have had little practical significance without an evaluation of the energy consumption associated with the motor required to rotate the building under study. To this end, a calculation was performed under the assumption that the house is supported by three wheels running on a circular rail, enabling it to rotate about its vertical barycentric axis. Considering the geometry (rail radius of 7 m), the weight of the house (98 t), the low coefficient of friction between the steel wheel and the rail (0.001), and the small angular velocity (0.0000727 rad/s), the power requirements are very modest (approximately 5 W), and the annual energy consumption does not exceed 50 kWh.

With regard to costs relative to a static house, the rotation system (i.e., the steel structure as a whole, the wheels, and the motor) results in an increase of slightly more than 3%. The total cost of the system is approximately 6,000€.

The simplifying hypotheses were:

- The building is constructed using a CLT system (E_0 = 11,000 N/mm²; fire resistance rating: 90 minutes; u = 12%; $R'_w \geq 50$ dB; $L'_{n,w} < 63$ dB; $D_{2m,nT,w} > 45$ dB; U = 0.18 W/m²K).
- Double-glazed windows with argon gas filling and timber frames (U_w = 1.4 W/m²K).
- Layout of the rooms considering the living room as a reference space.
- Rectangular geometry with an aspect ratio of 1:2 (8,66 m × 17,32 m) and h = 3 m.
- Flat roof.
- Specific weight of wood ρ_0 = 500 kg/m^3 (average value for larch).
- Imposed load on floors: 200 kg/m^2.
- A very short time to reach steady-state angular velocity was assumed (1 s).
- The same power was assumed for acceleration to the target speed and for maintaining it.
- The imposed load was assumed to be concentrated on the perimeter walls.

The gains constitute a contribution to the heating of the rooms in the winter period while, in the summer period, they determine a contribution to the cooling of the same rooms.

To all this must be added the further energy gains that can be obtained with a monocrystalline photovoltaic system with a power of 3 kW$_P$ and a solar thermal system with collectors of 5 m^2 of collector area, located on the roof of the house with an optimized tilt angle in relation to the location. The phenomena that influence the irradiation of a building and, in particular, of a part of it, are many and multifaceted and must be dealt with in depth for a correct evaluation of the energy inputs and for their optimisation, in relation to the needs depending on location and seasonal variation.

The considerations set out above constitute the starting point for the present study.

The project was developed in various phases, so that the feasibility of each of them served as the starting point for subsequent phases, thereby ensuring their potential to deliver meaningful results, and excluding, while also ensuring that the practical non-applicability of what had been determined up to that moment, would not reduce the study to a mere theoretical question.

For this reason, the first step was carried out by comparing the energy incident on the static walls outside the Earth's atmosphere, at more than 120 km from the ground, with that incident on the dynamic surface. The coordinates of Genoa were considered as a reference.

Initially, an equation was derived that allows the calculation of the angle of incidence for dynamic walls. For this purpose, by referring to a single wall and rotating it at a speed equal to the apparent speed of the Sun, it was imposed, in the formula that allows the determination of the angle of incidence, that the azimuthal angle γ coincides with that of the Sun (ψ)

This condition corresponds to the fact that the wall is always facing the Sun.

The conditions under which an azimuthal offset between the two rotations must be imposed are discussed below.

The following equation was derived from the above:

$$\cos(\theta) = \sin(\Phi) \cdot \cos\left[\arcsin\left(\frac{\sin\omega \cdot \cos\delta}{\cos h}\right)\right] \cdot \cos(\delta) \cdot \cos(\omega) + \\ + \sin\left[\arcsin\left(\frac{\sin\omega \cdot \cos\delta}{\cos h}\right)\right] \cdot \cos(\delta) \cdot \sin(\omega) + \\ - \cos(\Phi) \cdot \cos\left[\arcsin\left(\frac{\sin\omega \cdot \cos\delta}{\cos h}\right)\right] \cdot \sin(\delta) \quad (2)$$

(2), in combination with (1), and taking into account all that has been explained in the introduction, has made it possible to evaluate the irradiation on a solar tracking wall, with a zero azimuthal offset between the wall and the Sun, a condition which is appropriate during the coldest periods of the year.

The study was carried out taking into consideration individual walls which, taken together, constitute the external envelope of a building.

This building, as previously indicated, is assumed to have a rectangular plan, a geometry which implies that the perimeter walls are orthogonal in pairs.

However, this simplification is overcome by the final equations obtained and by the methodology adopted, which allows the development of the project regardless of the geometric characteristics of the building envelope or, moreover, of the RES systems installed on it, which may have different orientations.

For the evaluation of the static conditions, the vertical surfaces were oriented to the east, south, and west.

Returning to the building envelope, the actual heat transfer through a wall depends on various factors, including the type of material and the thickness of the surface, the temperature difference between its inner and outer faces, and the heat exchange conditions.

In this phase, in order to avoid excessive calculations, reference was made to the part of the surface facing the outside of the building, comparing the results both in absolute terms and in percentage terms, with the assumption that these results provide a sufficiently accurate proxy for the values obtained after heat transfer through the wall.

Furthermore, the surface was considered as a whole, regardless of differences between opaque and transparent areas.

To address the second phase of the project, which concerns the study within the Earth's atmosphere, the subsequent evaluations were carried out using experimental data from ENEA (Agenzia nazionale per le nuove tecnologie, l'energia e lo sviluppo economico sostenibile, Italy). This agency collected and processed data on global solar radiation at ground level on a horizontal plane for 242 locations in Italy over a 17-years period (ENEA, 2023).

In the project, 21 locations were taken into consideration. They are distributed throughout the country, so as to cover the various climatic characteristics present in Italy, i.e., located in the north, centre, south, mountain, hill, and coastal areas, as well as the coldest and hottest sites in the country.

Finally, the monthly mean values of daily solar radiation incident on a horizontal surface $\overline{H}$ are known.

Table 1 indicates the main characteristics of the 11 locations that are most representative of the various Italian climatic conditions.

Table 1. Characteristics of the selected locations.

	Latitude	Altitude (m)	Degree days	Italian Climate Zone	T min (°C) (average)	T max (°C) (average)
Aosta	45° 44′14″ N	583	2.850	E	−3.2	26.7
Venezia	45° 26′ 23″ N	2.56	2.345	E	1.1	27.8
Milano	45° 28′ 01″ N	138	2.404	E	−0.9	29.2
Genova	44° 24′ 26″ N	18	1.435	D	5	27
Bologna	44° 29′ 38″ N	54	2.259	E	0.1	30.4
Firenze	43° 46′ 17″ N	50	1.821	D	1.4	31.1
Roma	41° 53′ 35″ N	21	1.415	D	2.1	31.7
Napoli	40° 50′ 09″ N	17	1.034	C	4	33
Palermo	38° 06′ 56″ N	14	751	B	8.9	30.5
Livigno	46° 32′ 17″ N	1.816	4.648	F	−8	19
Lampedusa	45° 44′ 14″ N	−0.025	568	A	12	29

With the values of $\overline{H}$ and those of $\overline{H}_0$ (monthly mean value of daily solar radiation incident on a horizontal surface outside the Earth's atmosphere) calculated for the chosen locations, the value of the $\overline{K}_h$ cloudiness index for the twelve months of the year for each site was determined.

The next step was to calculate, for each location and each month of the year, the fraction of scattered radiation $\frac{\overline{H}_d}{\overline{H}}$, both with Liu-Jordan's and Page's models. Subsequently, with these values, the monthly mean of the daily scattered solar radiation $\overline{H}_d$ was determined, using the aforementioned models and the results were compared.

For subsequent evaluations, Liu and Jordan's model was adopted, which proved to be more suitable for the locations considered.

The values determined in this phase were for horizontal surfaces.

In order to perform more general calculations, i.e., for any inclination of the wall and for any azimuth angle, it was necessary to determine the relative transformation factor R_b, taking into account the complications discussed above.

Having made these considerations, a first comparison was made by comparing the result of the calculations obtained with (2), for a solar tracking vertical wall with zero azimuth offset between γ and ψ, with those for three vertical fixed walls facing E, S, and W.

Even under these conditions, we were faced with the problems previously anticipated because Klein's equation does not admit solutions for vertical walls (β=90°).

Furthermore, for each location analysed, additional problems were found when the angle γ exceeded certain values for the various months of the year.

To overcome these problems and obtain valid results, the calculation of the global radiation and its components was carried out numerically.

To simplify the procedure, given that monthly mean values are used, it is possible to obtain results characterized with good accuracy by referring to a particular day of each month (Klein, 1977).

For all the cases under study, the daily and monthly irradiation values was calculated.

At this point, the Liu and Jordan's model was used to obtain the results within the Earth's atmosphere.

In particular, the monthly average values of the daily radiation were calculated, for each of the three components direct, diffuse from the sky and reflected from the ground, as well as the corresponding global radiation.

In addition, for a complete evaluation, the monthly and annual values of solar radiation were calculated. These data allowed the comparison between the various conditions and the determination of the corresponding energy gains.

At the end of this phase, the analysis of the hottest periods of the year was undertaken / we addressed the hottest periods of the year.

In this case, the goal is to cool the building's rooms. To mitigate this need and, consequently, the associated use of energy-consuming systems, it is necessary to reduce the heating of the walls as much as possible.

For this reason, it is necessary that the walls, which correspond to the rooms most inhabited during the day, be exposed as little as possible to the solar radiation.

The solution was to offset the angle of the walls with respect to solar radiation, i.e. to identify the most appropriate azimuth angle offset between the azimuth of the Sun and that of the wall in question.

In the study, for the rotating wall, simulations were carried out with various values of the azimuth angle offset ($\psi - \gamma$) by performing the same calculations described above for the solar tracking wall also for these conditions. In particular, azimuth offsets of ±20°, ±70° and ±90° were initially taken into account.

Figure 5 shows these conditions applied to the studied house model.

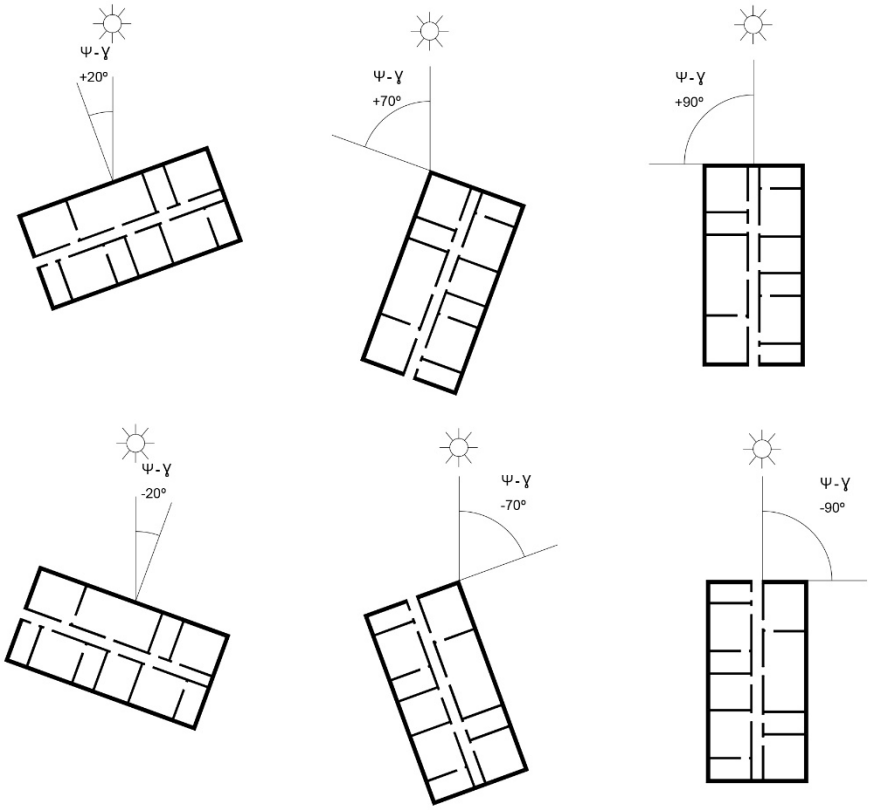

Figure 5. Summer azimuth offsets applied to the home model.

This method can also be used to optimize the benefits of natural ventilation in buildings. The driving force of natural ventilation, given by the pressure difference between any two points across the building envelope, depends on the building's aspect ratio and its orientation (Ferrucci, 2018). The ability to manage the latter parameter is a further contribution in this respect, thereby improving energy savings and indoor comfort.

It should be noted that the simulations were carried out by comparing the optimal rotation of the building with an ideal building whose walls are arranged according to the orientation described initially, without going into the details of the best exposure of a static building. On the other hand, buildings are not always, nor can they always be designed, with optimal arrangements in relation to the apparent movement of the Sun.

In this regard, the importance of correctly distributing spaces and organizing their activities is emphasized, and avoiding common errors that lead to unnecessary energy consumption (Ansari, 2018).

In this phase as well, the results, obtained numerically, allowed the verification of the actual energy gains.

A final evaluation was carried out considering the real case of the detached house taken as a reference in the previous calculations and, specifically, for the rotating wall, the facade corresponding to the most frequently occupied rooms was used as the reference surface. Due to its size, its length is twice that of the perpendicular façades.

Considering the overall dimensions indicated above, the area of the reference façade measures 51.96 m^2. With respect to this façade, the results obtained with the Liu and Jordan method were applied.

Subsequently, in order to resolve the theoretical incompatibilities indicated above and to obtain solutions through an analytical method, a new reference system was imposed and the following final expression was reached:

$$\cos(\theta) = \cos(\beta) \cdot \sin(h) + [\sin(\beta) \cdot \cos(h)] \cdot [\cos(\psi - \gamma)] \quad (3)$$

which, for example, for a rotating wall with rotational speed and azimuth equal to those of the Sun, is simplified into:

$$\cos(\theta) = \sin(h + \beta) \quad (4)$$

considerably simpler and more elegant than (2).

At the end of the computational phase, a calculation program was created using the VBA of Excel, in order to enhance the possibility of performing simulations of various types and to develop further future studies.

3. Results and Discussion

As previously mentioned, the study was developed in subsequent steps. The first evaluation was performed outside the Earth's atmosphere and involved the comparison between the energy incident on a solar tracking wall, with zero azimuth offset between the azimuths of the Sun and the surface under study (the dynamic wall), and that incident on three fixed walls oriented towards E, S, and W. It should be noted that the calculations refer to the external surfaces of the walls. In this phase, real energy gains were already observed / were already evident.

The values of monthly average daily solar radiation (Wh m^{-2} day^{-1}), relating to each of the coldest months of the year for each of the four types of surfaces, show that there are substantial differences, to the detriment of energy saving, between each of the "static" and dynamic surfaces (Table 2).

Table 2. Monthly Average Daily Solar Radiation Values (Wh m^{-2} day^{-1}).

	Dynamic wall	**Static wall S**	**Δ%**	**Static wall E**	**Δ %**	**Static wall O**	**Δ %**
September	14.051	6.781	−107	5.388	−161	5.365	−162
October	13.372	8.883	−51	4.351	−223	4.329	−225
November	12.413	9.668	−28	3.389	−315	3.368	−317
December	11.803	9.705	−22	2.923	−381	2.903	−384
January	12.215	9.765	−25	3.192	−340	3.172	−343
February	13.200	9.382	−41	4.049	−247	4.026	−249
March	14.014	7.834	−79	5.075	−177	5.052	−178

It can also be seen that, for the east and west-facing walls, the energy reductions compared to the dynamic one are more pronounced in the colder months, contrary to what happens for the south-facing wall. The latter, moreover, generally has better irradiation conditions than the other two fixed walls. The percentage differences range from a minimum of 22%, for the static south-facing surface in December, to a maximum of 384%, for the static west-facing surface in December.

At this point, an evaluation was made of the consumption of the motor having the function of rotating the building. Using the building characteristics reported in the previous paragraph (which also allow the adopted simplifications to be verified), the motor consumption was found to be negligible compared to the gains. Actually, given the very small angular velocity involved ($7.27 \cdot 10^{-5}$ rad/s in the case of complete rotation of the building), the power required for the movement was extremely limited. The condition of complete rotation of the building, in reality, is only required in the period between the spring and autumn equinoxes, when the angle between sunrise and sunset is greater than 180°. For energy purposes, in the remaining period of the year, once the Sun has set, it is more convenient to have the building rotate in reverse, thereby covering a shorter angular distance.

After an initial rough assessment, the project took into account the real-world conditions within the Earth's atmosphere.

Going into the details of the results of the calculations, it should be noted that, during the development of the project, ENEA continued its work of measuring and processing data relating to solar

radiation. For the purpose of a correct analysis, it is important to point out that, in February 2022, the values were obtained from a multi-year average for the period 2006-2020. In September 2023, the new values relate to the average calculated over the period 2006-2022 (ENEA, 2023).

It is interesting to note that, by adding just two years of measurements and averaging over 17 years, substantial increases have been obtained in general, and in particular for the locations considered in the present project.

For the latter, the average annual percentage change ranges from a minimum of 5% to a maximum of more than 17% (Figure 6).

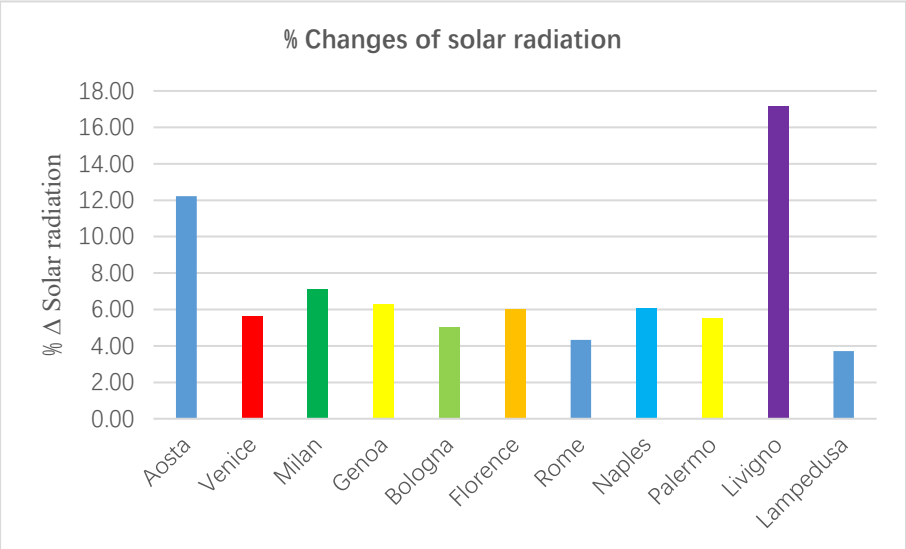

Figure 6. % changes in annual solar radiation in the period 2006-2022 compared to 2006-2020.

In particular, by analysing the larger percentage changes distributed over the twelve months of the year (Table 3), it was verified that, for colder locations, the increases are more pronounced. Similar results are obtained by considering the coldest periods when comparing the coldest and hottest periods of the year.

Table 3. % changes in solar radiation in the period 2006-2022 compared to 2006-2020.

	Jan	**Feb**	**Mar**	**Apr**	**May**	**June**	**Jul**	**Aug**	**Sept**	**Oct**	**Nov**	**Dec**
Aosta	23.07	20.42	17.58	14.62	11.27	8.55	7.25	8.61	11.53	13.94	18.99	17.86
Venice	11.68	9.72	10.54	6.98	5.05	4.68	2.02	3.24	5.53	7.87	8.78	6.35
Milan	12.52	11.46	11.23	8.28	6.88	6.01	4.08	4.83	7.31	7.56	10.24	8.84
Genoa	10.49	9.27	10.56	7.64	6.41	5.46	3.81	3.70	6.50	6.75	8.79	5.37
Bologna	9.19	9.80	9.89	6.26	4.73	4.26	2.00	2.50	4.59	6.51	6.65	4.04
Florence	8.84	9.52	10.88	6.81	5.62	5.46	3.45	3.86	5.33	7.31	8.42	5.29
Rome	8.10	8.22	6.63	3.67	3.34	2.74	2.50	2.63	4.67	7.39	7.30	6.86
Naples	8.00	9.81	7.97	6.31	5.66	5.40	5.04	4.65	5.82	6.91	6.36	7.66
Palermo	8.18	9.89	4.49	4.01	3.20	4.77	5.49	5.52	6.01	6.74	6.67	9.86
Livigno	29.39	28.03	33.56	24.93	15.99	12.99	9.66	11.12	16.55	20.73	23.80	23.74
Lampedusa	5.59	6.22	2.06	0.91	1.73	3.64	4.36	4.26	3.41	4.78	5.88	7.68

Given this premise, the average cloudiness index $\overline{K}_h$ was calculated using both the Liu-Jordan's and Page's methods.

The first observation that can be made concerns the variations due to the update of the ENEA data: for reasons strictly related to the definition of this parameter, the increases of $\overline{K}_h$ related to the two different periods correspond directly to those previously presented for $\overline{H}$. The second observation concerns the results obtained with Page's method, which are systematically higher to those of Liu and Jordan's.

The next step was the calculation of the diffuse radiation fraction $\frac{\overline{H}_d}{\overline{H}}$. As already mentioned, the above methods were applied here as well.

From the analysis of the results, it can be observed that, following the ENEA update, the parameters computed with both methods decreased. This effect is due to the presence, in the equations of the two models, of negative terms that include $\overline{K}_h$. In almost all conditions and locations, the decreases are more evident for Page's model, with a maximum of −22% in Aosta in February.

Then the study determined the values of daily diffuse solar radiation $\overline{H}_d$, as well as the direct, reflected, and global components of daily solar radiation and the global one. It is possible to make a final assessment related to the variation of the data measured at the sites: the direct and reflected components have undergone noticeable increases, especially in the colder months, whereas the diffuse component has shown limited variation on average.

For the final evaluations, Liu and Jordan's model was preferred to Page's model. The choice was made following a comparison between the values obtained using the two models. The data obtained by calculating the diffuse radiation from the sky using Page's method were systematically higher than those obtained by the other method.

Calculations have shown that the diffuse component represents, in the coldest months (Oct-Mar), about 10% of the total and, in the warmest months (Apr-Sep), during which an azimuth offset of 90° was imposed between the rotating wall and the Sun exceeds 70% (Table 4).

Table 4. Ratio between diffuse and global component of solar radiation (%).

	Jan	**Feb**	**Mar**	**Apr**	**May**	**June**	**Jul**	**Aug**	**Sept**	**Oct**	**Nov**	**Dec**
Aosta	7.9	7.94	9.57	76.47	77.51	76.31	74.52	74.81	74.59	8.69	8.18	7.50
Venice	10.02	10.52	10.78	76.68	76.58	74.96	74.07	74.94	76.10	10.28	11.11	10.76
Milan	8.68	10.10	10.44	76.89	76.80	75.20	73.41	74.73	75.73	11.10	11.05	10.18
Genoa	9.79	10.84	11.65	77.21	76.70	75.11	73.40	74.31	75.63	11.11	10.80	11.18
Bologna	9.73	10.25	11.35	77.25	77.05	75.20	74.17	74.48	76.29	10.46	10.94	9.70
Florence	9.60	10.61	12.01	77.14	77.08	75.01	73.22	73.69	75.89	10.35	10.20	10.68
Rome	8.86	9.53	11.59	75.86	75.22	73.10	71.14	71.93	75.15	9.75	9.39	8.28
Naples	9.56	10.35	11.83	75.44	74.39	72.46	70.82	71.43	74.48	9.85	10.21	8.69
Palermo	9.75	10.80	12.11	75.30	73.73	71.78	70.02	71.23	75.57	10.88	9.74	9.54
Livigno	14.12	17.93	17.85	80.23	79.51	78.02	77.65	77.85	77.33	9.49	11.87	14.38
Lampedusa	8.53	9.27	10.45	73.80	72.32	70.89	69.69	70.86	74.25	10.25	8.99	8.65

Given that the aim of the project is to evaluate, also in absolute terms, the energy gain using a rotating building, so as to determine, among other things, the economic feasibility of the option, for precautionary reasons, as a precautionary measure, Liu and Jordan method was preferred.

Analysing the variations of the daily diffuse solar radiation $\overline{H}_d$ following the update mentioned above, it can be seen that, due to the presence in its calculation of the factors $\overline{H}$ (increased) and $\frac{\overline{H}_d}{\overline{H}}$ (decreased), the updated values are slightly lower than the previous ones (Table 5).

Table 5. Changes in monthly average of the daily diffuse radiation – Liu and Jordan model – kWh m^{-2} day^{-1} (2006-2022 compared to 2006-2020).

	Jan	**Feb**	**Mar**	**Apr**	**May**	**June**	**Jul**	**Aug**	**Sept**	**Oct**	**Nov**	**Dec**	**TOT**
Aosta	−0.004	−0.022	−0.044	−0.041	−0.028	−0.040	−0.058	−0.053	−0.054	−0.022	−0.001	0.002	−0.030
Venice	0.005	−0.001	−0.019	−0.024	−0.023	−0.038	−0.022	−0.075	−0.021	−0.006	0.005	0.004	−0.018
Milan	0.002	−0.003	−0.024	−0.025	−0.027	−0.044	−0.047	−0.035	−0.029	−0.003	0.006	0.005	−0.019
Genoa	0.003	−0.001	−0.014	−0.022	−0.027	−0.042	−0.045	−0.031	−0.028	−0.004	0.004	0.003	−0.017
Bologna	0.003	−0.003	−0.017	−0,018	−0,019	−0,033	−0,021	−0,021	−0,017	−0.006	0.003	0.001	−0.012
Florence	0.002	−0.003	−0.013	−0.021	−0.021	−0.043	−0.043	−0.038	−0.022	−0.008	0.002	0.003	−0.017
Rome	−0.002	−0.011	−0.016	−0.020	−0.025	−0.037	−0.047	−0.038	−0.025	−0.015	−0.002	−0.002	−0.020
Naples	−0.001	−0.009	−0.018	−0.035	−0.049	−0.075	−0.091	−0.069	−0.037	−0.016	−0.001	−0.002	−0.033
Palermo	−0.003	−0.011	−0.014	−0.026	−0.035	−0.076	−0.109	−0.083	−0.029	−0.014	−0.005	−0.001	−0.034

Livigno	0.03 6	0.05 5	0.06 0	0.01 5	−0.0 03	−0.0 24	−0.0 25	−0.0 21	−0.0 25	−0.0 12	0.02 1	0.02 8	0.00 9
Lamped usa	−0.0 11	−0.0 25	−0.0 17	−0.0 10	−0.0 27	−0.0 70	−0.0 94	−0.0 72	−0.0 26	−0.0 19	−0.0 12	−0.0 09	−0.0 33

Analysing the diffuse component, as seen above, acquires considerable importance in the hottest months, during which it accounts for more than 70% of the radiation incident on the rotating wall.

The calculation related to $\bar{R}_b$ represented the most difficult aspect from a mathematical point of view.

Its value is fundamental for the direct component of solar radiation on an inclined surface relative to the horizontal plane within the atmosphere.

Taking into account the equation relating to the calculation of $\bar{H}_{bh}$, a number of considerations can be made. The first is that a greater value of $\bar{R}_b$, under the same conditions of $\bar{H}$ and $\bar{H}_d$, determines a greater value of the direct component. The second is that a greater value of $\bar{H}_d$ determines a lower value of $\bar{H}_{b\beta}$.

The direct component is dominant compared to the diffuse and reflected component ($\bar{H}_{r\beta}$), therefore it is desirable to have higher values of the direct component in the coldest periods of the year. The opposite is true for warmer periods. The $\bar{H}_{b\beta}$ and $\bar{H}_{r\beta}$ components are not entirely independent of surface orientation and depend, in addition to its inclination, respectively, on $\bar{H}_d$ and the reflectivity of the soil $\rho \cdot \bar{H}$. Their contribution, therefore, is the same for any vertical wall only if orientation-dependent terms are neglected or held constant.

Analysing the $\bar{R}_b$ data for the colder months, the advantages, in percentage, of a solar tracking wall compared to a fixed one oriented to the south, vary between 20% and 100% (Table 6).

Table 6. % differences between $\bar{R}_b$ of the rotating wall compared to the fixed wall facing south.

	Jan	**Feb**	**Mar**	**Oct**	**Nov**	**Dec**
Aosta	23.40	39.38	76.50	48.69	26.79	20.21
Venice	23.63	39.41	76.96	48.83	27.10	20.36
Milan	23.65	39.40	76.92	48.81	27.11	20.39
Genoa	24.76	40.50	78.60	49.85	27.98	21.22
Bologna	24.34	40.49	77.68	49.81	28.03	21.31
Florence	25.26	41.59	79.64	50.71	28.63	21.57
Rome	26.48	43.50	83.56	53.43	30.25	23.29
Naples	27.34	44.82	85.62	54.71	31.35	23.91
Palermo	29.95	47.94	92.18	58.56	33.57	26.15
Livigno	22.64	51.56	74.75	47.33	26.32	19.67
Lampedusa	32.02	51.46	99.52	62.87	36.19	28.37

The advantages are even more evident when compared with fixed east- or west-facing walls (Table 7).

Table 7. % differences between $\bar{R}_b$ of the rotating wall compared to the fixed walls oriented to the east or west.

	Jan	**Feb**	**Mar**	**Oct**	**Nov**	**Dec**
Aosta	293.97	232.00	180.61	213.08	275.48	316.75
Venice	292.37	230.41	179.95	211.87	274.28	314.59
Milan	292.66	230.56	180.01	211.98	274.52	314.94
Genoa	288.01	227.37	177.68	208.82	269.75	308.54
Bologna	287.42	227.84	176.69	209.18	270.51	309.64
Florence	284.91	226.48	176.29	207.42	267.40	304.45
Rome	275.24	220.73	173.07	203.42	259.77	295.19
Naples	270.56	218.01	170.75	200.54	256.07	289.17
Palermo	259.93	209.96	165.54	193.64	245.09	276.35
Livigno	297.93	265.81	181.46	214.21	279.79	322.24
Lampedusa	249.06	202.99	160.60	187.48	236.10	265.17

In Figure 7 and 8, the total energy gains (sum of the three components mentioned above) are shown for both the coldest and warmest periods.

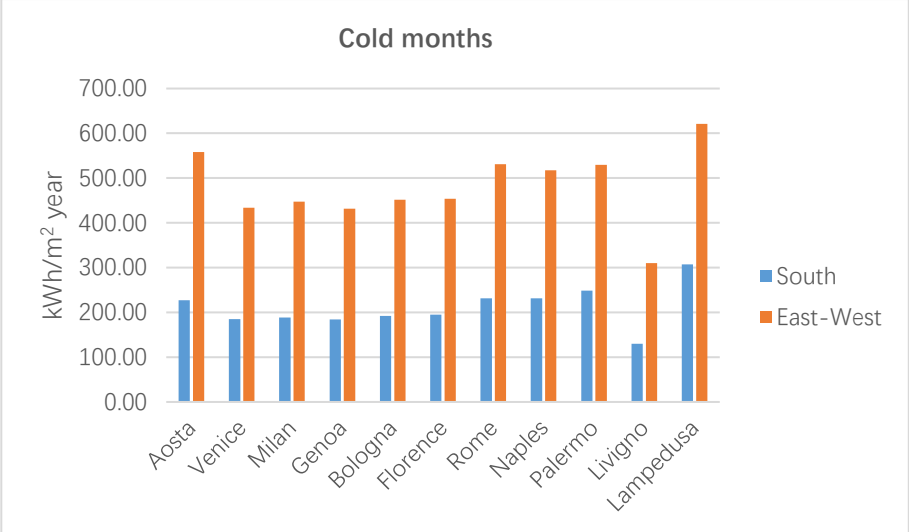

Figure 7. Solar radiation gains for rotating wall compared to fixed ones (cold months).

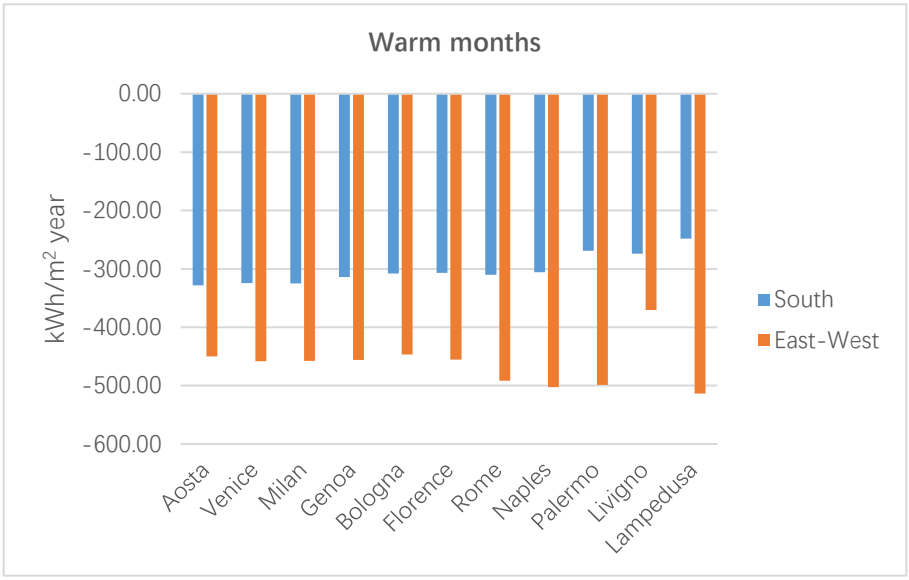

Figure 8. Solar radiation gains per rotating wall compared to fixed ones (warm months).

It should be remembered that the low values of the global radiation, for the solar tracking wall in the hottest months, are determined by imposing an azimuth offset of 90° relative to the azimuth of the Sun. This solution helps reduce the cooling demand of the rooms the need for room cooling.

The advantage of the first solution over the others is evident.

The total gains obtained over the entire calendar year were also calculated, through a higher energy input in the coldest months, contributing to space heating, and a lower one in the warmer ones, contributing to the need for cooling (Figures 9 and 10).

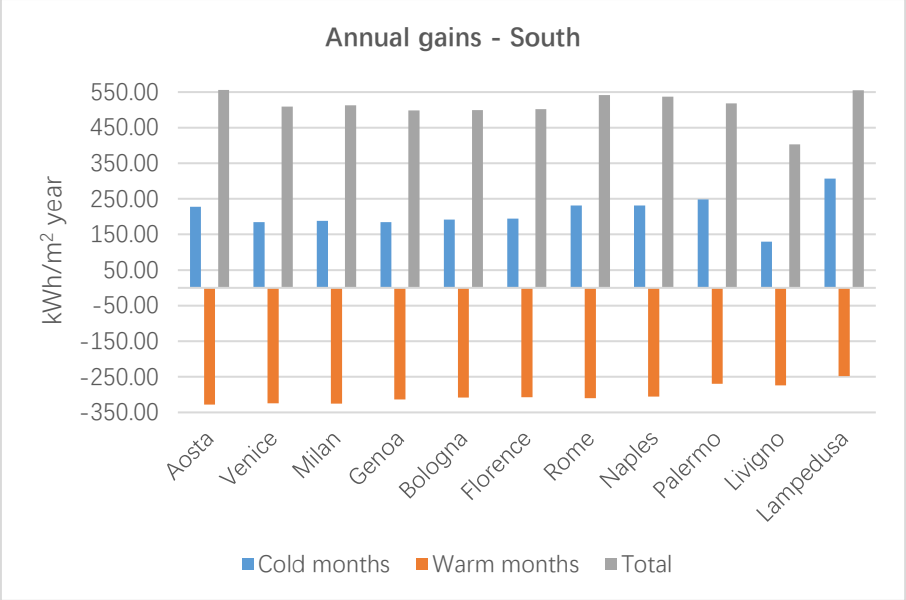

Figure 9. Annual solar radiation gains for rotating versus fixed south-facing walls.

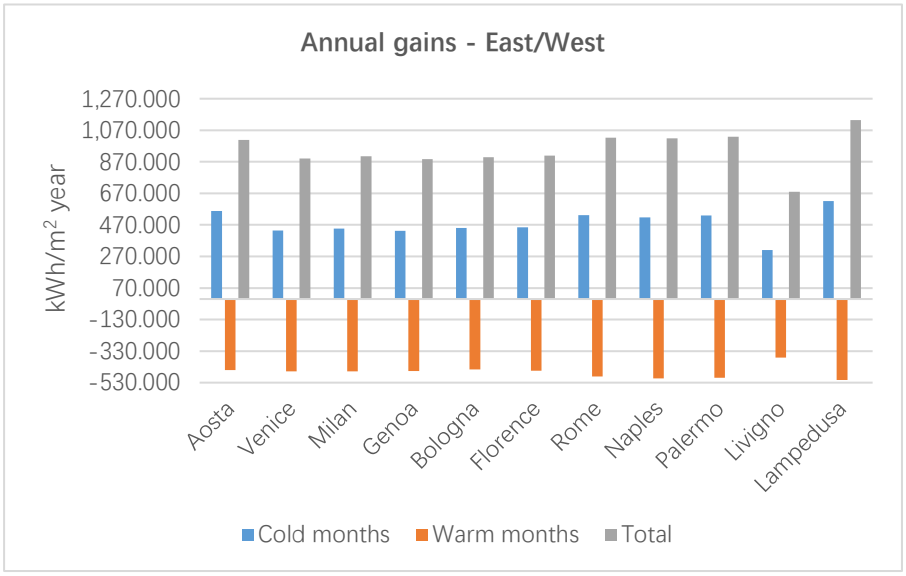

Figure 10. Annual solar radiation gains for rotating wall versus fixed east/west facing.

Finally, the results obtained above were applied to the rotating wall of the real building described above, in order to determine the energy gain and estimate the real cost-effectiveness of the option. The specifications of rotation and azimuth offset related to the solar azimuth are those mentioned above. The surface area of the reference façade measures 51.96 m^2 (Table 8).

Table 8. Annual global radiation gains (kWh/y) for real wall (51.96 m^2) compared to fixed walls.

	South	**East-West**
Aosta	28,877.42	52,406.50
Venice	26,455.01	46,319.19
Milan	26,669.24	47,027.98
Genoa	25,904.66	46,116.25
Bologna	25,968.53	46,677.49
Florence	26,079.71	47,246.46
Rome	28,132.52	53,156.95
Naples	27,910.36	52,978.65
Palermo	26,914.89	53,432.27

Livigno	20,963.26	35,347.73
Lampedusa	28,859.36	58,937.39

As it is easy to observe, the gains are substantial, corresponding to more than 2,000 kg per year of LPG or 2,000 m^3 of natural gas compared with the south-facing wall, and about 5,000 kg per year of LPG or 5,000 m^3 of natural gas in the case of east- or west-facing walls.

For a broader assessment, it is necessary to take into account the losses or gains that the two walls perpendicular to the rotating wall experience compared to the fixed walls oriented to the east and west. Considering that the diffuse and reflected components are assumed to be independent of orientation, the only component that comes into play is the direct one. For the above considerations, the walls at 90° from the rotating one are never exposed to this component, both in the cold and in the hot months. The comparison can therefore be made by analysing its calculated values for the east and west-facing walls. These data must be distinguished in relation to the period of the year: in the cold months, energy gains contribute to the heating of the rooms and represent an advantage; in the hot ones, whereas in the warm months, they represent an increase in the cooling demand (Tables 9 and 10).

Table 9. Direct component for east- and west-facing walls (cold months) – kWh/m^2 day.

	Jan	**Feb**	**Mar**	**Oct**	**Nov**	**Dec**	**Tot**
Aosta	0.98	1.48	2.00	1.59	0.98	0.77	7.79
Venice	0.69	1.12	1.80	1.36	0.71	0.52	6.20
Milan	0.80	1.17	1.85	1.25	0.71	0.56	6.35
Genoa	0.75	1.13	1.71	1.30	0.77	0.54	6.20
Bologna	0.75	1.20	1.75	1.38	0.76	0.63	6.48
Florence	0.80	1.19	1.68	1.43	0.86	0.59	6.54
Rome	0.97	1.43	1.81	1.61	1.03	0.89	7.73
Naples	0.94	1.36	1.82	1.64	0.99	0.90	7.65
Palermo	1.06	1.42	1.87	1.61	1.18	0.95	8.09
Livigno	0.42	0.50	0.98	1.43	0.61	0.33	4.26
Lampedusa	1.36	1.78	2.24	1.82	1.41	1.19	9.79

Table 10. Direct component for east- and west-facing walls (warm months) – kWh/m^2 day.

	Apr	**May**	**June**	**Jul**	**Aug**	**Sept**	**Tot**
Aosta	2.25	2.28	2.55	2.80	2.59	2.28	14.75
Venice	2.22	2.43	2.77	2.86	2.64	2.08	15.00
Milan	2.18	2.39	2.73	2.96	2.59	2.13	14.99
Genoa	2.12	2.39	2.71	2.94	2.64	2.14	14.93
Bologna	2.12	2.33	2.70	2.82	2.61	2.05	14.63
Florence	2.13	2.31	2.71	2.94	2.71	2.10	14.91
Rome	2.31	2.58	2.95	3.17	2.91	2.20	16.11
Naples	2.36	2.68	3.01	3.18	2.95	2.28	16.45
Palermo	2.35	2.72	3.02	3.19	2.93	2.13	16.34
Livigno	1.64	1.93	2.26	2.29	2.11	1.91	12.14
Lampedusa	2.53	2.85	3.06	3.16	2.93	2.30	16.82

As can be seen, the gains that are obtained in the rotating wall(s) due to a lower need for cooling in the warm months are greater than the losses that occur in the coldest months due to the increase in the energy needed for heating.

No specific assessment is provided for the wall parallel to the rotating wall, relative to the fixed north-facing wall. In fact, for cooling purposes, only diffuse and reflected radiation, assumed to be independent of orientation, act on this surface. Furthermore, these are the only ones that affect the rotating wall, given its azimuth offset, therefore the comparison is not meaningful.

At the end of this analysis, some evaluations were performed regarding the solar systems located on the rotating building.

As regards photovoltaic solar systems, there are various types of solar trackers: one or two degrees of freedom (Caffarelli, 2012; Alomar, 2023). In relation to the study, it is appropriate to refer to one degree of freedom (yaw trackers), i.e. azimuth tracking. They are the ones which can take advantage of being fixed to the building and, at the same time, while also exploiting the rotation of the structure in order to produce more energy. Theoretically, the use of the other types cannot be excluded, but the potential energy benefits do not justify the additional technical complexity. The use of azimuth trackers is quite

common, and measured energy production data demonstrate gains of 20-25% compared to fixed systems (Caffarelli, 2012). For a more accurate evaluation, calculations were performed in the project, for a 3 kW_P photovoltaic system, using the Photovoltaic Geographic Information System (PVGIS) (JRC 2012). The results indicate the annual energy production (kWh) for fixed photovoltaic panels, with an optimized tilt angle and with azimuth equal to zero, and for solar tracking panels around a vertical axis and, also in this case, with an optimized tilt angle (Table 11).

Table 11. Annual energy produced by a 3 kW_P photovoltaic plant.

	Fixed	Solar tracker	Gain (%)	Gain (kWh)
Aosta	3,718.62	4,701.02	26.42	982.40
Venice	4,027.26	5,226.62	29.78	1,199.36
Milan	4,003.04	5,209.68	30.14	1,206.64
Genoa	4,090.93	5,357.59	30.96	1,266.66
Bologna	4,001.70	5,248.23	31.15	1,246.53
Florence	4,037.26	5,344.41	32.38	1,307.15
Rome	4,457.69	5,866.31	31.60	1,408.62
Naples	4,460.84	5,804.01	30.11	1,343.17
Palermo	4,547.72	5,959.51	31.04	1,411.79
Livigno	3,169.63	3,785.13	19.42	615.50
Lampedusa	Data are lacking			

It is possible to observe that, excluding only the case of Livigno, the gains are on average around 30%. The values, expressed in kWh, are even more significant. It is clear from these values that, by properly designing the photovoltaic system, it is possible, with the surplus of energy obtainable from rotation, not only to make up for the consumption due to the electric motor that moves the building, but also to contribute to building's electricity demand.

A similar assessment can be carried out for solar thermal systems, which are now widely installed in new buildings.

In short, the results obtained indicate that the gains that can be obtained from the designed choice constitute a real basis for practical developments.

In light of the above, it is interesting to put forward some indications for future studies, which could make a further contribution to the energy improvement of buildings:

- Optimization of the azimuth angle offset between rotating walls and the Sun by conducting simulations using a larger set of angular values.
- Evaluation of heat transfer through the walls by accounting for the actual surface temperatures on both faces over the entire calendar year.
- Application of the radiation laws for the appropriate use of:
    - assessment of surface selectivity (materials and colours), including differentiated surface properties across façades, in order to identify the optimal associated conditions.
    - verification of the applicability of polarization-related laws to provide an additional contribution to managing wall temperatures during the summer period.
- Optimization of the thermal phase shift in relation to the movement of the building.
- Optimization of the building's rotation strategy to enhance natural ventilation, with the aim of effectively harnessing external air currents.
- Application of the study to site-specific climatic conditions, including the analysis of environmental scenarios more extreme than those considered in the present work.
- Study of the effects due to the presence of external obstacles.
- For multi-storey buildings, assessment of differentiated rotation across levels, analysing the specific conditions arising from the distinct housing characteristics of each floor.

4. Conclusions

The challenges arising from energy production and consumption, including climate change, environmental degradation, adverse impacts on human health, and geopolitical coercion, demand integrated solutions that build upon and improve existing approaches. This research project sought to identify the conditions and physical–technical parameters governing solar radiation on the façades of a timber building equipped with a solar-tracking system, with the aim of reducing overall energy demand. To this end, a method was developed to calculate (i) the solar energy transmitted through building

envelopes and (ii) the potential energy gains achievable by optimizing the rotational motion of buildings relative to the Sun's apparent trajectory.

The study focused on rotating buildings, which have traditionally served primarily aesthetic purposes, and demonstrated that appropriately selected rotational speeds and azimuth offsets can yield substantial performance benefits. Specifically, optimized rotation can reduce energy requirements for both summer cooling and winter heating while simultaneously increasing on-site renewable generation from photovoltaic and solar-thermal systems.

Twenty-one locations across Italy were examined to represent the country's full range of climatic conditions. The theoretical framework was subsequently applied to a representative case study: a 150 m², 450 m³ single-family timber house sited in each location. Estimated annual gains averaged above 26,000 kWh relative to a fixed south-oriented façade and above 50,000 kWh relative to east- and west-oriented façades, excluding the coldest site and prior to accounting for rotational motor energy. For a 3 kWp photovoltaic system, rotating configurations produced, on average, approximately 30% higher yields than fixed systems, with comparable improvements for solar thermal. These findings suggest that solar-tracking buildings can meaningfully advance energy efficiency and renewable production where technically and economically feasible.

Author Contributions

The first author conducted the research presented in this manuscript as part of the doctoral thesis currently being undertaken at UCAM Universidad Católica de Murcia.
The second author, a professor at Universitat Politècnica de València, serves as the principal supervisor of the study and oversees the doctoral candidate's thesis.

Conflict of Interest Statement

No potential conflict of interest was reported by authors.

Data Availability Statement

The data that support the findings of this study are available from the corresponding author, [GC], upon reasonable request.

References

Alomar, O.R., Ali, O.M., Ali, B.M., Qader, V.S. and Ali, O.M. (2023) 'Energy, exergy, economical and environmental analysis of photovoltaic solar panel for fixed, single and dual axis tracking system: an experimental and theorical study', Case Studies in Thermal Engineering, 51, 103635. Available at: https://doi.org/10.1016/j.csite.2023.103635

Ansari, S., Larsen, G.D. and Shao, L. (2018) 'Identifying energy savings opportunities for a multi-use venue building', *Future Cities and Environment*, 4, 12. Available at: https://doi.org/10.5334/fce.9

Arieti, F. (2021) Progettare edifici a energia zero. Santarcangelo di Romagna: Maggioli Editore.

Bahan, I. (2016) 'The Round House Wilton'. Available at: https://roundhousewilton.com/about/

Caffarelli, A., De Simone, G., Stizza, M. and D'Amato, A. (2012) Sistemi solari fotovoltaici. Santarcangelo di Romagna: Maggioli Editore.

Carbonari, A., Scarpa, M. and Méndez Plaza, F.I. (2025) 'Environmental control of urban covered courtyards in Mediterranean climates: comparison between different strategies', Energy Catalyst, 1, pp. 22–34. Available at: https://doi.org/10.61552/EC.2025.002

Cerizzi, M. (2024) 'Le 5 case rotanti più famose al mondo'. Available at: https://www.deabyday.tv/casa-e-fai-da-te/riparazioni/article/1463/Le-5-case-rotanti-pi--famose-al-mondo.html

Cucumo, M.A., Martinelli, V. and Oliveti, G. (1994) Ingegneria solare: principi ed applicazioni. Bologna: Pitagora Editrice.

DIIS (Danish Institute for International Studies) (2024) 'Energy as a weapon – decoding blackmail tactics in Europe'. Available at: https://www.diis.dk/en/research/energy-as-a-weapon-decoding-blackmail-tactics-in-europe

Duffie, J.A. and Beckman, W.A. (2013) Solar engineering of thermal processes. Hoboken, NJ: John Wiley & Sons. Available at: https://doi.org/10.1002/9781118671603

ENEA (Agenzia nazionale per le nuove tecnologie, l'energia e lo sviluppo economico sostenibile) (2023) 'Atlante solare della radiazione solare'. Available at: http://www.solaritaly.enea.it/TabelleRad/TabelleRadIt.php

European Union (2021) Directive 2010/31/EU of the European Parliament and of the Council of 19 May 2010 on the energy performance of buildings (consolidated text 01/01/2021). Available at: https://eur-lex.europa.eu/legal-content/EN/TXT/?uri=CELEX%3A02010L0031-20210101

Eve, L. (2014) 'Rotating Girasole home follows the Australian sun'. Available at: https://inhabitat.com/rotating-girasole-home-follows-the-australian-sun/

Ferrucci, M., Brocato, M. and Peron, F. (2018) 'Digital tools for the morphological design of naturally ventilated buildings', Future Cities and Environment, 4, 9. Available at: https://doi.org/10.5334/fce.4

Galfetti, A., Frampton, K. and Farinati, V. (2014) Villa Girasole: la casa rotante / The Revolving House. Cinisello Balsamo (MI): Silvana Editoriale.
Goswami, Y.D. (2015) Principles of solar engineering. Boca Raton, FL: CRC Press.
Grassi, W. (2015) La gestione dell'energia solare e l'efficienza energetica degli edifici. Vol. 2 of Termoenergetica dell'Edificio. Santarcangelo di Romagna: Maggioli Editore.
Hottel, H.C. (1976) 'A simple model for estimating the transmittance of direct solar radiation through clear atmospheres', Solar Energy, 18(2), pp. 129–134. Available at: https://doi.org/10.1016/0038-092X(76)90045-1
IPCC (2023) Climate Change 2023: Synthesis Report. Geneva: IPCC. Available at: https://www.ipcc.ch/report/sixth-assessment-report-cycle/
Iqbal, M. (1983) An introduction to solar radiation. New York: Academic Press. Available at: https://doi.org/10.1016/B978-0-12-373750-2.X5001-0
JRC (2012) 'Photovoltaic Geographical Information System (PVGIS) – European Commission'. Available at: https://re.jrc.ec.europa.eu/pvg_tools/en/
Klein, S.A. (1977) 'Calculation of monthly average insulation on tilted surfaces', Solar Energy, 19(4), pp. 325–329. Available at: https://doi.org/10.1016/0038-092X(77)90001-9
Lazzarin, R. (1981) Sistemi solari attivi. Padova: Franco Muzio & C. Editore.
Lazzarin, R. and Rossetto, L. (1980) 'Insolazione su superfici inclinate: modelli matematici e dati sperimentali', in Atti del XXXV Congresso Nazionale ATI. St. Vincent, pp. 263–276.
Liu, B.Y.H. and Jordan, R.C. (1960) 'The interrelationship and characteristic distribution of direct, diffuse and total solar radiation', Solar Energy, 4(3), pp. 1–19. Available at: https://doi.org/10.1016/0038-092X(60)90062-1
Liu, B.Y.H. and Jordan, R.C. (1961) 'Daily insolation on surfaces tilted toward the equator', ASHRAE Transactions, pp. 526–541.
Mazzucchelli, E.S. (2016) Sistemi costruttivi in legno: tecnologie, soluzioni e strategie progettuali verso edifici Zero Energy. Santarcangelo di Romagna: Maggioli Editore.
McLaughlin, K. (2023) 'La casa rotante più famosa del mondo è in vendita a 5,3 milioni di dollari'. Available at: https://www.ad-italia.it/article/casa-rotante-in-vendita-san-diego/
Nagy, Z. et al. (2022) 'Adaptive building envelopes for solar energy optimization: a review of design, control and modeling approaches', Renewable and Sustainable Energy Reviews, 165, 112509.
Ottolenghi, M. (2025) 'Quadrant House, versione contemporanea della casa rotante'. Available at: https://www.cosedicasa.com/ristrutturare/quadrant-house-versione-contemporanea-della-casa-rotante-64303
Our World in Data (2020) 'Coal consumption'. Available at: https://ourworldindata.org/grapher/coal-consumption-by-country-terawatt-hours-twh
Our World in Data (2020) 'Coal proved reserves'. Available at: https://ourworldindata.org/grapher/coal-proved-reserves
Our World in Data (2020) 'Gas consumption'. Available at: https://ourworldindata.org/grapher/gas-consumption-by-country
Our World in Data (2020) 'Gas proved reserves'. Available at: https://ourworldindata.org/grapher/natural-gas-proved-reserves
Our World in Data (2020) 'Oil consumption'. Available at: https://ourworldindata.org/grapher/oil-consumption-by-country
Our World in Data (2020) 'Oil proved reserves'. Available at: https://ourworldindata.org/grapher/oil-proved-reserves
Our World in Data (2020) 'Years of fossil fuel reserves left, 2020'. Available at: https://ourworldindata.org/grapher/years-of-fossil-fuel-reserves-left?time=2020
Page, J.K. (1961) 'The estimation of monthly mean values of daily total short-wave radiation on vertical and inclined surfaces from sunshine records for latitudes 40°N–40°S', in Proceedings of the United Nations Conference on New Sources of Energy, 35(S), p. 98.
Suman, S., Calautit, J.K., Wei, S. et al. (2025) 'Assessing the energy-saving potential of passive strategies in commercial buildings in the top upcoming megacities', Energy Catalyst, 1, pp. 1–21. Available at: https://doi.org/10.61552/EC.2025.001
Taut, B. (1929) Modern Architecture. London: The Studio Limited.
Ward, S. (2012) 'Modern Homes Los Angeles'. Available at: https://modernhomesla.blogspot.com/2012/11/the-dangelo-house-futuristic-desert.html
Zhang, S., Xu, Q. and Riffat, S. (2025) 'Multi-objective optimization of environmental retrofits in eldercare buildings: a case study in Suzhou', Green Technology Innovation, 2025. Available at: https://doi.org/10.36922/gti.7807
Zhu, Y. (2025) 'Carbon neutrality strategy and advancements in China's building sector', Global Decarbonisation, 2025. Available at: https://doi.org/10.17184/eac.9639